frequency for the detection of CCO, the C–C stretch, is weak in the infrared spectrum of clusters, so electron energy loss spectroscopy is a more promising technique than infrared for the detection of CCO on metal surfaces.

Acknowledgment. This research was supported by the Department of Energy Sciences Program, Grant no. DE-FG02-86ER13640.

Molecular Dynamics of the Primary Photochemical Event in Bacteriorhodopsin. Theoretical Evidence for an Excited Singlet State Assignment for the J Intermediate

Robert R. Birge,* Leonore A. Findsen, and Brian M. Pierce

Department of Chemistry, Carnegie Mellon University Pittsburgh, Pennsylvania 15213

Received March 23, 1987

The nature of the primary photochemical event in light-adapted bacteriorhodopsin (bR) has been studied by a variety of experimental[1-10] and theoretical[11] techniques. The picosecond time resolved absorption studies[5] are interpreted generally in terms of Scheme I. Raman,[6] FTIR,[7] NMR,[8] and optical[9] studies indicate

Scheme I

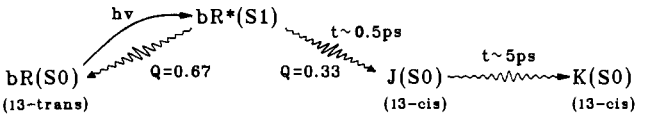

Scheme II

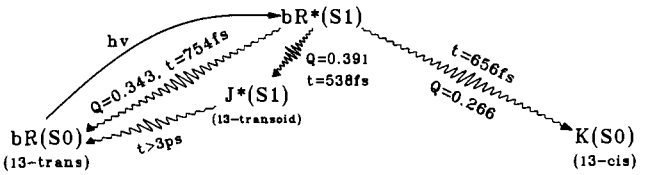

that K is an isomerized (13-cis) species. It is inferred that the chromophore in J is isomerized (13-cis) and that relaxation and/or proton translocation generates K.[2,3,5,11]

We studied the primary event in bacteriorhodopsin by using INDO-PSDCI SCF-MO theory and semiempirical molecular dynamics theory. Our procedures are identical with those used previously to study rhodopsin.[12-14] We generated our models of bR (Figure 1a) and K (Figure 1b) by using molecular orbital theory to predict bR and K absorption spectra and energy differences and optimizing the structures to best reproduce the experimental data.[9,10a] The calculated potential surfaces, Franck–Condon absorption maxima and photoisomerization dynamics associated with the absorption of light, are shown in Figure 1c–f. The shape of the lowest lying excited singlet state potential surface, however, is far from optimum for dynamic coupling into the ground state. The S_1 surface has a positive hump at the 270° ΔE_{10} minimum which reduces dramatically the coupling efficiency (see Discussion in ref 12 and 13). This characteristic of the S_1 surface was observed in all of our calculations, irrespective of model, and differs significantly from the corresponding feature calculated for the S_1 surface of rhodopsin.[11c-13] The rhodopsin S_1 surface has a relatively deep potential well at the ΔE_{10} surface minimum which traps the trajectory in an activated complex resulting in excellent dynamic coupling into the ground state.[12,13] This difference in potential surfaces results in a rhodopsin → bathorhodopsin quantum yield (0.62)[12] which is roughly twice that calculated for the bR → K phototransformation (0.27; see below).

Our calculations predict complex dynamics and biphasic repopulation of bR involving three pathways depopulating the S_1^* potential surface (Scheme II). Only one pathway leads to a vibrationally relaxed 13-cis ground-state species in 656 fs (λ_{max} = 621 nm, Q = quantum yield = 0.266). A second dynamic pathway regenerates vibrationally relaxed bR in 754 fs (λ_{max} = 559 nm, Q = 0.343). The third pathway populates a metastable 13-transoid excited singlet state species in 538 fs (λ_{max} = 650 nm, Q = 0.391). This population decays via nondynamic processes to reform bR exclusively (Figure 1e). We label this species "J" for reasons outlined below.

Calculated transient one-photon absorption spectra of the ensemble of excited species are shown in Figure 1g. These spectra were generated by using oscillator strength weighted Gaussian wavepacket propagation theory,[15] a basis set consisting of the 16 lowest lying excited singlet states and a 300 fs Gaussian excitation pulse. We assumed that the time constant for decay of the trapped S_1 species (Figure 1e) was 6 ps based on model compound studies.[9c] Individual components or component mixtures are responsible for

(1) For relevant Reviews see 2–4.
(2) Ottolenghi, M. *Adv. Photochem.* **1980**, *12*, 97–200.
(3) Birge, R. R. *Annu. Rev. Biophys. Bioeng.* **1981**, *10*, 315–54.
(4) Stoeckenius, W.; Bogomolni, R. *Annu. Rev. Biochem.* **1982**, *52*, 587–616.
(5) (a) Polland, H.-J.; Franz, M. A.; Zinth, W.; Kaiser, W.; Kölling, E.; Oesterhelt, D. *Biophys. J.* **1986**, *49*, 651–662. (b) Sharkov, A. V.; Pakulev, A. V.; Chekalin, S. V.; Matveetz, Y. A. *Biochim. Biophys. Acta* **1985**, *808*, 94–102. (c) Petrich, J. W.; Breton, J.; Martin, J. L. *Biophys. J.* **1987**, *51*, 416a. (d) Ippen, E. P.; Shank, C. V.; Lewis, A.; Marcus, M. A. *Science (Washington, DC)* **1978**, *200*, 1279–1281; Shichida, Y.; Matuoka, S.; Hidaka, Y.; Yoshizawa, T. *Biochim. Biophys. Acta* **1983**, *723*, 240–246. (e) Kaufmann, K. J.; Rentzepis, P. M.; Stoeckenius, W.; Lewis, A. *Biochem. Biophys. Res. Commun.* **1976**, *68*, 1109–1115; Kaufmann, K. J.; Sundstrom, V.; Yamane, T.; Rentzepis, P. M. *Biophys. J.* **1978**, *22*, 121–124. Applebury, M. L.; Peters, K. S.; Rentzepis, P. M. *Biophys. J.* **1978**, *23*, 375–382.
(6) Smith, S. O.; Lugtenburg, J.; Mathies, R. A. *J. Membr. Biol.* **1985**, *85*, 95–109. Smith, S. O.; Myers, A. B.; Pardoen, J. A.; Winkel, C.; Mulder, P. P. J.; Lugtenburg, J.; Mathies, R. *Proc. Natl. Acad. Sci. U.S.A.* **1984**, *81*, 2055–2059; Braiman, M.; Mathies, R. *Proc. Natl. Acad. Sci. U.S.A.* **1982**, *79*, 403–407; Aton, B.; Doukas, A. G.; Callender, R. H.; Becher, B.; Ebrey, T. G. *Biochemistry* **1977**, *16*, 2995–2999. Stockburger, M.; Klusmann, W.; Gattermann, H.; Massig, G.; Peters, R. *Biochemistry* **1979**, *18*, 4886–4900. Hsieh, C.-L.; Nagumo, M.; Nicol, M.; El-Sayed, M. A. *J. Phys. Chem.* **1981**, *85*, 2714–2717. Terner, J.; Hsieh, C.-L.; Burns, A. R.; El-Sayed, M. A. *Proc. Natl. Acad. Sci. U.S.A.* **1979**, *76*, 3046–3050.
(7) Rothschild, K. J.; Roepe, P.; Gillespie, J. *Biochim. Biophys. Acta* **1985**, *808*, 140–147. Bagley, K.; Dollinger, G.; Eisenstein, L.; Singh, A. K.; Zimanyi, L. *Proc. Natl. Acad. Sci. U.S.A.* **1982**, *79*, 4972–4976. Siebert, F.; Mäntele, F. *Eur. J. Biochem.* **1983**, *130*, 565–573.
(8) Harbison, G. S.; Smith, S. O.; Pardoen, J. A.; Courtin, J. M. L.; Lugtenburg, J.; Herzfeld, J.; Mathies, R. A.; Griffin, R. G. *Biochemistry* **1985**, *24*, 6955–6962.
(9) (a) Goldschmidt, C. R.; Ottolenghi, M.; Korenstein, R. *Biophys. J.* **1976**, *16*, 839–843. Hurley, J. B.; Ebrey, T. G. *Biophys. J.* **1978**, *22*, 49–66. Goldschmidt, C. R.; Kalisky, O.; Rosenfeld, T.; Ottolenghi, M. *Biophys. J.* **1977**, *17*, 179–183. (b) Oesterhelt, D.; Hess, B. *Eur. J. Biochem.* **1973**, *37*, 316–326. (c) Polland, H.-J.; Franz, M. A.; Zinth, W.; Kaiser, W.; Kölling, E.; Oesterhelt, D. *Biochim. Biophys. Acta* **1984**, *767*, 635–639. Fang, J.-M.; Carriker, J. D.; Balogh-Nair, V.; Nakanishi, K. *J. Am. Chem. Soc.* **1983**, *105*, 5162–5164. Kölling, E.; Gärtner, W.; Oesterhelt, D.; Ernst, L. *Angew. Chem. Int. Ed Engl.* **1984**, *23*, 81–82. (d) Kouyama, T.; Kinosita, K.; Ikegami, A. *Biophys. J.* **1985**, *47*, 43–54. Iwasa, T.; Tokunaga, F.; Yoshizawa, T. *Biophys. Struct. Mech.* **1980**, *6*, 253–270.
(10) (a) Birge, R. R.; Cooper, T. M. *Biophys. J.* **1983**, *42*, 61–69. (b) Ort, D. R.; Parson, W. W. *Biophys. J.* **1979**, *25*, 355–364.
(11) (a) Dinur, U.; Honig, B.; Ottolenghi, M. *Photochem. Photobiol.* **1981**, *33*, 523–527. (b) Schulten, K.; Tavan, P. *Halobacterium halobium. Nature (London)* **1978**, *272*, 85–86. Tavan, P.; Schulten, K. *Biophys. J.* **1986**, *50*, 81–89. (c) Birge, R. R.; Pierce, B. M. In *Photochemistry and Photobiology*; Zewail, A., Ed.; Hardwood Academic: New York, 1982; Vol. 2, pp 841–855.
(12) Birge, R. R.; Hubbard, L. M. *J. Am. Chem. Soc.* **1980**, *102*, 2195–2205. Birge, R. R.; Hubbard, L. M. *Biophys. J.* **1981**, *34*, 517–534.
(13) Birge, R. R. In *Biological Events Probed by Ultrafast Laser Spectroscopy*; Alfano, R. R., Ed.; Academic Press: New York, 1982; pp 299–317.
(14) The vibrational relaxation rate parameter ($|\Delta E_{vib}/\Delta t|_{avg}$) was set equal to 5 eV·ps^{-1} and the density of states factor (ρ) was set equal to 2 eV^{-1}. These parameters were adjusted upward (toward increased vibrational relaxation) until wavelength-independent quantum yields were observed (see ref 12 and 13). Test calculations indicate that the principal conclusions of this study are invariant to reasonable changes in parameterization.
(15) Tannor, D. J.; Heller, E. J. *J. Chem. Phys.* **1982**, *77*, 202–218. Birge, R. R.; Pierce, B. M. *Int. J. Quant. Chem.* **1986**, *29*, 639–656.

0002-7863/87/1509-5041$01.50/0

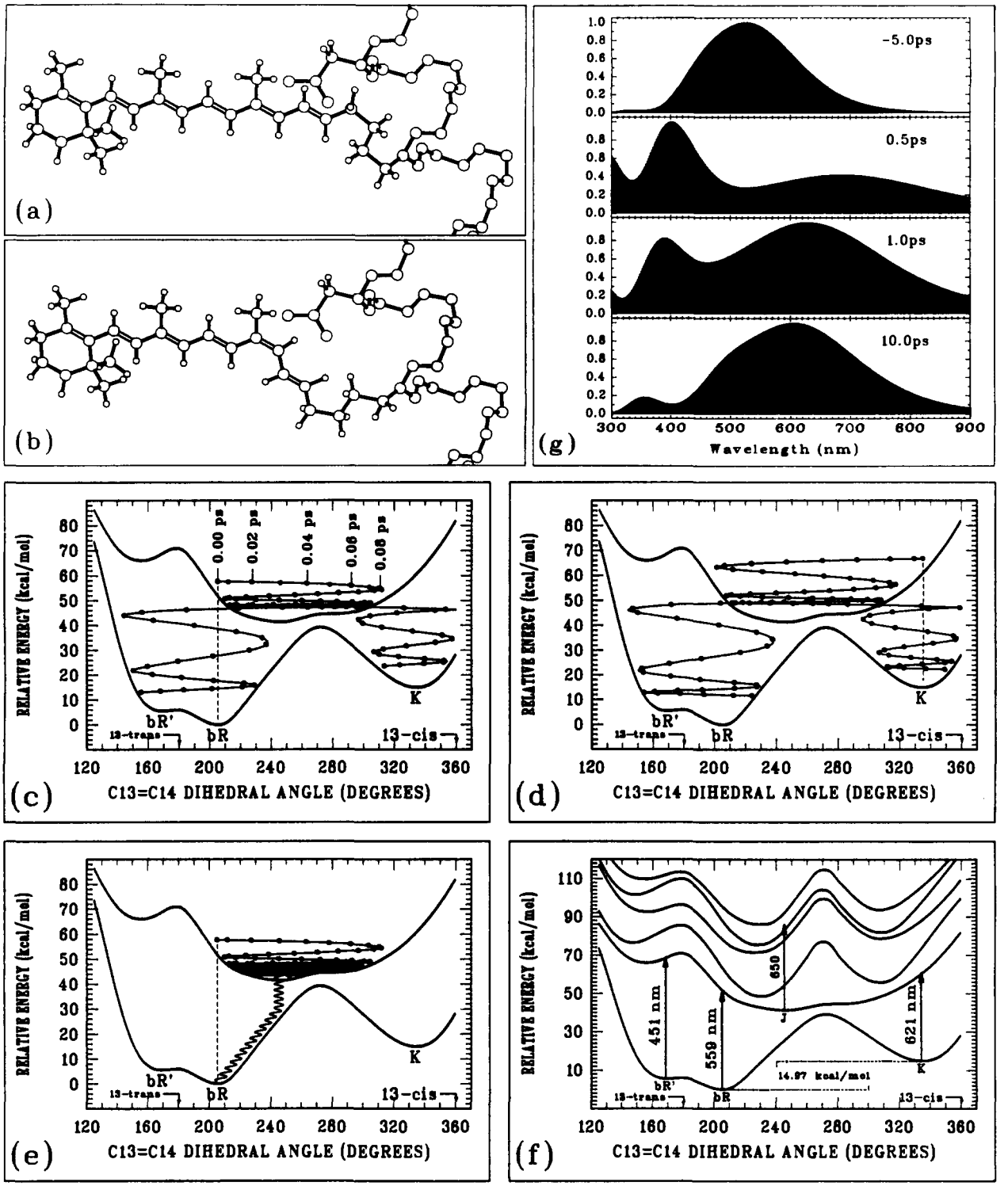

Figure 1. Molecular dynamics of the primary photochemical transformations of light-adapted bacteriorhodopsin. The assumed structure of light-adapted bacteriorhodopsin (bR) is shown in a, and the assumed structure of the primary photoproduct K is shown in b. The calculated (INDO-PSDCI) potential surfaces, the Franck–Condon absorption maxima, and the photoisomerization dynamics associated with the absorption of light are shown in c–e. The dots along the trajectories (c, d, and e) mark time increments of 0.01 ps. The two trajectories that are of primary importance in depopulating the excited singlet state by dynamic processes are shown for the forward and reverse photoreactions in c and d, respectively. Approximately 40% of the excited-state species are trapped in the first excited singlet state potential minimum ($\Phi_{13,14} \simeq 245°$) and must decay to reform bR via less efficient, nondynamic processes (e). Franck–Condon maxima associated with the various ground- and excited-state minima are shown in f, and the time-resolved one-photon absorption spectra of the ensemble for 300 fs laser excitation (corrected for ground-state bR absorption for 0.5, 1.0, and 10.0 ps) are shown in g. Note that the spectra are made up of mixtures of species based on the following approximate prescriptions: −5 ps (pure bR), 0.5 ps (mostly hot S_1^*), 1.0 ps (mixture K and J), 10.0 ps (pure K).

the transient absorption: −5 ps (pure bR), 0.5 ps (mostly hot S_1^*), 1.0 ps (mixture of J and K), 10.0 ps (pure K). The strong transient absorption band predicted at ~400 nm (Figure 1g, 0.5 ps) correlates reasonably well with the transient band observed at ~460 nm by Petrich et al.[5c] We predict that both the J ($S_1 \rightarrow S_4, S_5$) and K ($S_0 \rightarrow S_1$) absorption spectra have very similar absorption maxima and are polarized similarly (±7°) in agreement with transient absorption[5a-d] and polarization[5b] studies.

We interpret the observation of a ~30-nm red-shifted species in <1 ps[5] to rapid population of a metastable excited state pop-

ulation J (τ = 538 fs) simultaneously with K (τ = 656 fs) (Scheme II). Relatively slow decay of J back to bR results in the apparent generation of a more blue-shifted intermediate (Δt = 10 ps, Figure 1g). Time resolved resonance Raman spectroscopy has the potential of detecting J and testing the validity of our model. Furthermore, the transition from J (S_1) to the ground state is potentially observable by using time resolved fluorescence spectroscopy. We predict this transition to be very broad ($\Delta\tilde{\nu} \approx \sim 6000$ cm^{-1}) with a Franck–Condon maximum at ~ 1.6 μ.

The Biosynthesis of LL-C10037α from the Shikimate Pathway

Yvonne G. Whittle and Steven J. Gould*[1]

Department of Chemistry, Oregon State University
Corvallis, Oregon 97331

Received September 29, 1986

LL-C10037α, an antitumor metabolite of *Streptomyces* LL-C10037 first assigned structure **1**,[2] has recently been shown to have the corrected structure **2**.[3] Several related structures have been isolated from a wide variety of microorganisms. For example, sarubicin A, **3**, contains a quinone moiety which we have shown to be derived from the shikimate metabolite 6-hydroxyanthranilic acid, **4**.[4] In addition, the hydroxyazaquinone **5**[5] is derived from shikimic acid **6** via *p*-aminobenzoic acid (PABA),[5,6] while chaloxone **7**,[7] isolated with its cometabolite methyl anhydroshikimic acid **8**,[8] may also be shikimate derived. On the other hand, the members of a large family of metabolites[9] represented by epoxydon, **9**,[10] have been clearly shown to be acetate-derived polyketides.[9,10] We now report evidence that **2** is derived via the shikimic acid pathway with 3-hydroxyanthranilic acid, **10**, as the key intermediate.

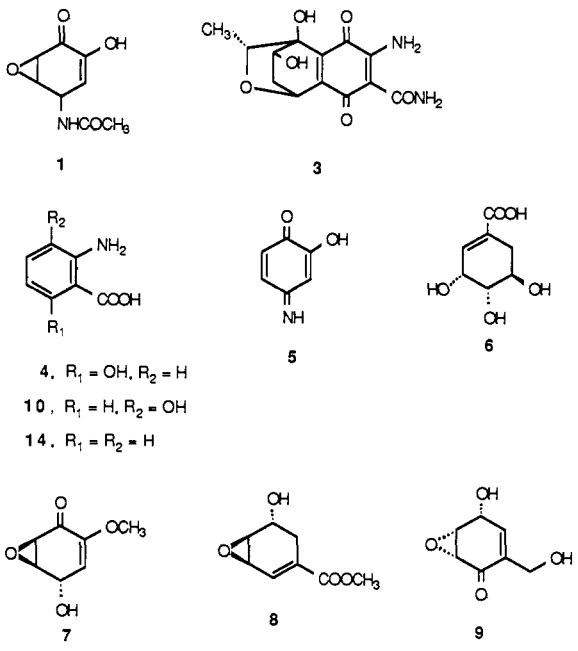

Cultures of *S.* LL-C10037 were grown in shake flasks (200 mL of broth in a 1-L Erlenmeyer) at 28 °C as previously described.[2] After incubation for 122 h, the broth was obtained free of the mycelia, adjusted to pH 4.7 (KH_2PO_4), and saturated with $(NH_4)_2SO_4$. Extraction with ethyl acetate, concentration in vacuo, and column chromatography (20 g silica gel 60, eluted with 20% hexanes in ethyl acetate) typically gave 30 mg of crystalline LL-C10037α which was then recrystallized from methanol.

For feeding experiments cultures were usually grown for 96 h before potential precursors were added in a sterile manner through a Millipore filter unit, and the broth was worked up after a total of 122 h. A mixture of sodium [1-^{14}C]acetate (9 μCi), **11a**, sodium acetate (23.6 mg), **11**, and sodium [2-^{13}C]acetate

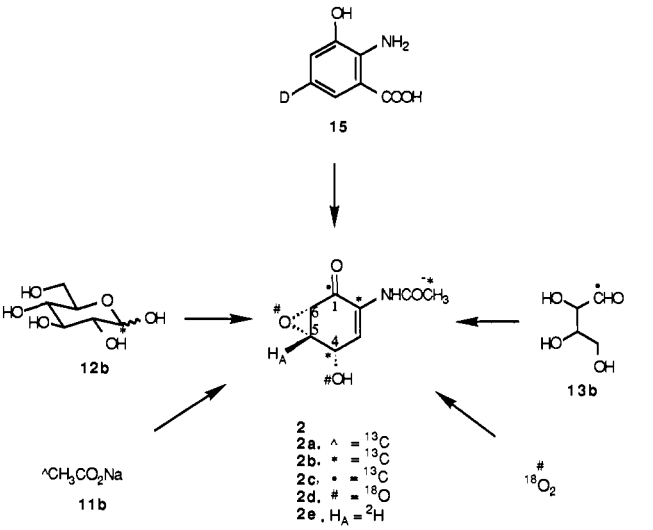

(68.3 mg), **11b**,[12] was fed first, and workup yielded 60 mg of **2a** (1.3% incorporation of ^{14}C). The 100.6-MHz ^{13}C NMR spectrum[13] of **2a** revealed enrichment (6.4%) only in the acetamide methyl group, revealing that the carbocycle is not polyketide in origin.

Feeding[14] a mixture of [1-^{14}C]-D-glucose, **12a**, (5.5 μCi) and [1-^{13}C]-D-glucose (0.996 g), **12b**,[15] yielded 35 mg of **2b**. The ^{13}C NMR spectrum of enriched **2b** showed labeling at C-2 (5.94%) and C-4 (7.02%), clearly indicative of a shikimate-type pathway;[16] the acetamide methyl was also enriched (4.69%), due to the incorporation of glycolysis-derived acetylCoA. The ring labeling pattern is inconsistent with the intermediacy of PABA (C-2 and C-6 would have been labeled in this case).[17]

To determine the correct orientation of the apparent shikimic

(1) Career Development Awardee of the National Cancer Institute (CA00880), 1979–1984.
(2) Lee, M. D.; Fantini, A. A.; Morton, G. O.; James, J. C.; Borders, D. B.; Testa, R. T. *J. Antibiot.* **1984**, *37*, 1149.
(3) Whittle, Y. G.; Keszler, D. A.; Gould, S. J., unpublished results of X-ray diffraction study. The absolute configuration shown in based on a circular dichroism study.
(4) Hillis, L. R.; Gould, S. J. *J. Am. Chem. Soc.* **1985**, *107*, 4593.
(5) Mize, P. D.; Jeffs, P. W.; Boekelheide, K. *J. Org. Chem.* **1980**, *45*, 3543.
(6) Tsuji, H.; Bando, N.; Ogawa, T.; Sasaoka, K. *Biochim. Biophys. Acta* **1981**, *667*, 326.
(7) Fex, T.; Trofast, J.; Wickberg, B. *Acta Chem. Scand., Ser. B* **1981**, *35*, 91.
(8) Fex, T.; Wickberg, B. *Acta Chem. Scand., Ser. B* **1981**, *35*, 97.
(9) Berdy, J. *Handbook of Antibiotic Compounds*; CRC Press Inc., 1980; Vol. 3 pp 343–366. Turner, W. B.; Aldridge, D. C. *Fungal Megabolites II*; Academic Press: New York, 1983; pp 62–67.
(10) Nabeta, K.; Ichihara, A.; Sakamura, S. *Agr. Biol. Chem.* **1975**, *39*, 409.
(11) Read, G.; Westlake, D. W. S.; Vining, L. D. *Can. J. Chem.* **1969**, *47*, 1071.
(12) [2-^{13}C]Sodium acetate (90 atom % C-13) was obtained from MSD Isotopes.
(13) Spectrum taken in 0.4 mL MeOH-d_4 with a Bruker AM 400 spectrometer at 100.6 MHz (sweep width = 2500 Hz, 64K data points, pulse width = 32.5°, acquisition time = 1.311 s, no. scans = 2839).
(14) In this experiment the production broth was harvested 193 h after inoculation.
(15) [1-^{13}C]-D-Glucose (99 atom % C-13) was obtained from Omicron Chemicals, Ithaca, NY.
(16) Haslam, E. *The Shikimate Pathway*; Halsted Press: New York, 1974; pp 8–9.
(17) Reference 16, pp 105–107.

0002-7863/87/1509-5043$01.50/0